Available online at www.sciencedirect.com
SCIENCE DIRECT
Journal of Sound and Vibration 295 (2006) 870–883
JOURNAL OF SOUND AND VIBRATION
www.elsevier.com/locate/jsvi

Theoretical study of moving force identification on continuous bridges

Tommy H.T. Chan*, Demeke B. Ashebo

Department of Civil and Structural Engineering, The Hong Kong Polytechnic University, Kowloon, Hong Kong

Received 8 December 2003; received in revised form 9 December 2004; accepted 27 January 2006
Available online 17 April 2006

Abstract

A method to identify moving forces on a continuous bridge has been developed in this paper. The bridge is modelled as a Bernoulli–Euler beam and the boundary value problem of the beam is solved to get the exact mode shape functions of the vibrating beam with intermediate supports. As the number of spans of the bridge increases, the identification accuracy decreases and at the same time more execution time is needed to finish one case study. To minimize this problem, a method has been developed to identify moving forces on a selected span of interest from the continuous bridge. The Singular Value Decomposition (SVD) of the coefficient matrix of the overdetermined equation is used in the solution. To evaluate the method, simulations of two moving forces on a continuous bridge and on one selected span from the continuous bridge are studied. White noise is added to the simulated bending moment and acceleration responses to study the effect of noise in moving forces identification problem for different numbers and arrangements of sensors. The results obtained from the simulation study show that the method is effective in identifying moving forces and acceptable results can be obtained.

1. Introduction

Information on truck axles and gross weights is an important factor in both bridge and pavement designs. Traditional methods used to acquire such information are expensive and subject to bias and have led to the development of Weight-in-Motion (WIM) techniques. Several methods of WIM systems have been developed (Davis and Sommerville [1], Peters, AXWAY [2] and CULWAY [3]), but these systems can only measure the static axle loads. However, dynamic axle loads are also important as they may increase road surface damage by a factor of 2–4 over that caused by static loads, Cebon [4]. Therefore, it is important to have a better understanding of the time histories of the axle loads rather than a single equivalent load per axle.

Four advanced methods of moving force identification on bridges have been developed and validated by the authors. Interpretive Method I by Chan and O'Conner [5], Interpretive Method II by Chan et al. [6], Time Domain Method (TMD) by Law and Chan [7], and Frequency Time Domain Method by Law and Chan [8]. Each of the four methods has been proved successful in identifying not only static equivalent axle forces but also their time variations.

*Corresponding author. Tel.: +852 2766 6061; fax: +852 2334 6389.
E-mail address: cetommy@polyu.edu.hk (T.H.T. Chan).

0022-460X/$ - see front matter
doi:10.1016/j.jsv.2006.01.059

The system can be used not only to acquire the field data to develop dynamic load expressions for bridge design but also to use the data for further study on the understanding of bridge–vehicle interaction and identifying the characteristics of vehicles which will cause least damage to a bridge and the pavement. A comparison study of the accuracy of the force identification using the four methods is carried out and it is found that the TDM gives the best results [9,10]. However, the methods can only be applied to simply supported bridges. In order to have a broader application it is necessary to extend the moving force identification system for continuous bridges.

In recent years, many researchers have studied the time history of the dynamic responses of the continuous beams due to moving vehicle wheel loads. Zhang et al. [11] used the assumed mode shape function to study the vibration behaviour of a non-uniform Bernoulli–Euler beam whilst Henchi et al. [12], used the finite element approach to obtain the exact mode shapes and frequencies. In addition, Dugush and Eisenberger [13] used the exact element method to determine the natural frequencies and mode shapes, and the solution is obtained by application of modal analysis and the direct integration method.

All the above methods are mainly concentrated on the forward problem, i.e. determination of the dynamic responses due to moving vehicle loads. However, in the present study the model is developed to analyse bridge dynamic responses and also the inverse problem of force identification from the dynamic responses of the continuous bridge is studied. The bridge is modelled as a Bernoulli–Euler beam continuously supported over the inner supports and simply supported at the outer supports. The boundary value problem of the beam is solved to get the exact mode shape functions of the vibrating beam. Attention is given to the development of TDM in applying for continuous supported bridges to identify moving forces from bending moment and acceleration responses of bridge. The TDM approach is used to study the time history of the structural responses caused by time-varying moving forces, which is the forward problem. In order to identify the time history of moving forces, the inverse problem has been studied. The new approach of identifying the time history of the interactive forces between the axles and bridge for one selected span at a time is introduced while the vehicle is moving across the whole bridge. The simulations of two time-varying forces moving over the bridge are used to evaluate the method. The simulation results show that the method is effective in identifying moving forces.

2. Theoretical model

As shown in Fig. 1, the bridge superstructure is modelled as a continuous beam with a total span length L, constant flexural stiffness EI, constant mass per unit length ρ and viscous proportional damping C. The beam is assumed to be an Bernoulli–Euler beam, in which the effects of shear deformation and rotary inertia are not taken into account.

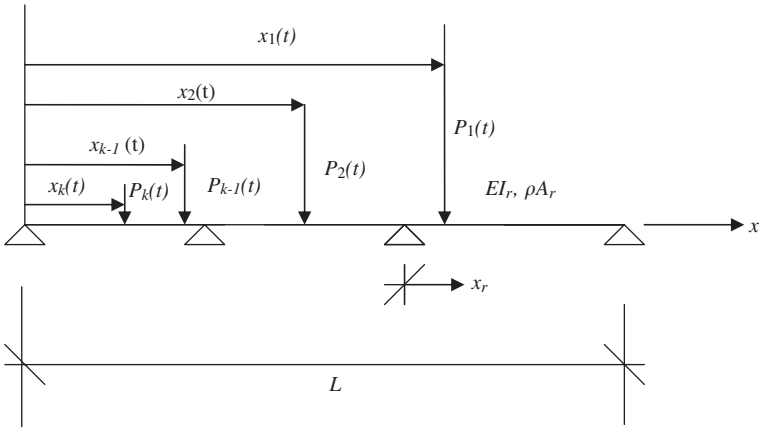

Fig. 1. Group of moving forces over the continuous beam.

Considering the group of forces $P_k(t)$ moving from left to right at a constant speed, the equation of motion can be expressed as

$$\rho \frac{\partial^2 v(x,t)}{\partial t^2} + C \frac{\partial v(x,t)}{\partial t} + \mathrm{EI} \frac{\partial^4 v(x,t)}{\partial x^4} = f(x,t). \tag{1}$$

Based on modal superposition, the solution of Eq. (1) can then be expressed as

$$v(x,t) = \sum_{n}^{\infty} \Phi_n(x) q_n(t), \tag{2}$$

where $q_n(t)$ is the nth modal amplitude and $\Phi_n(x)$ is the nth mode shape function of the beam. Substituting Eq. (2) into (1) and multiplying by Φ_n, integrating the resultant equation with respect to x between 0 and L and then applying orthogonality conditions, the equation of motion in terms of the modal displacement $q_n(t)$ is given as

$$\frac{\mathrm{d}^2 q_n(t)}{\mathrm{d}t^2} + 2\xi_n \omega_n \frac{\mathrm{d}q_n(t)}{\mathrm{d}t} + \omega_n^2 q_n(t) = \frac{1}{M_n} \sum_{k=1}^{N_l} \Phi_n(x_k(t)) f(x,t) \quad (n = 1, 2, \ldots, \infty), \tag{3}$$

where ω_n, ξ_n and M_n are modal frequency, damping ratio and modal mass of the nth mode, respectively, and

$$M_n = \int_0^L \rho A \Phi_n^2(x)\, \mathrm{d}x \tag{4}$$

for group of moving forces, $f(x, t)$ in Eq. (3) is given by Cebon [14]

$$f(x,t) = -\sum_{k=1}^{N_l} \delta(x - x_k(t)) p_k(t), \tag{5}$$

where $x_k(t)$ is the position of the kth force, and $\delta(t)$ the Dirac delta function.

3. Free vibration of the continuous beam

The modal shape function which is one of the components in Eqs. (2)–(4) should be determined beforehand in the process leading to the solutions. Substituting the modal expansion of Eq. (2) into (1) and ignoring the small damping term in Eq. (1), and then by separation of variables, the equation of the motion transforms to the fourth-order ordinary differential equation

$$\frac{\mathrm{d}^4 \Phi_n}{\mathrm{d}x^4}(x) - \lambda_n^4 \Phi_n(x) = 0. \tag{6}$$

For the rth span of the general case of a continuous beam as shown in Fig. 2, the solution of Eq. (6) is given by

$$\Phi_{nr}(x_r) = A_{nr} \sin(\lambda_{nr} x_r) + B_{nr} \cos(\lambda_{nr} x_r) + C_{nr} \sinh(\lambda_{nr} x_r) + D_{nr} \cosh(\lambda_{nr} x_r), \tag{7}$$

where $\Phi_{nr}(x_r)$ is the nth modal shape function of the rth span and x_r is the distance from the first support of the span under consideration.

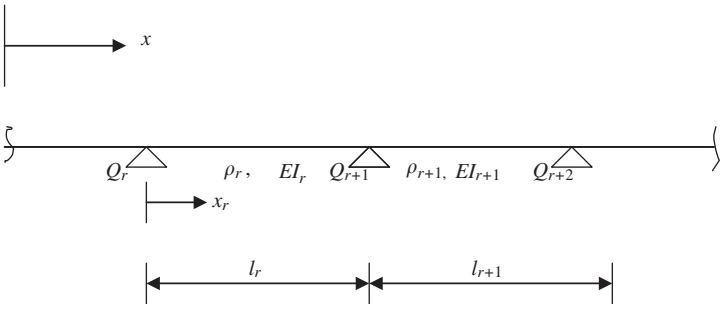

Fig. 2. General case of continuous beam.

In addition, λ_{nr} in Eq. (7) is the nth eigenvalue of the span r to be obtained from

$$\lambda_{nr} = \sqrt[4]{\frac{\rho_r \omega_n^2}{\mathrm{EI}_r}}, \tag{8}$$

where ρ_r and EI_r are mass per unit length and stiffness of the rth span respectively and ω_n is the nth natural frequency of the beam.

The total nth mode shape of the whole beam is given by

$$\Phi_n(x) = \Phi_{nr}(x_r), \quad \text{where } Q_r \leqslant x \leqslant Q_{r+1}. \tag{9}$$

The arbitrary constants A_{nr}, B_{nr}, C_{nr} and D_{nr} in Eq. (7) are determined from the boundary and initial conditions. The calculation of eigenfunctions is just a matter of substituting the appropriate boundary conditions in Eq. (7).

Eq. (7) applies to spans with arbitrary boundary conditions at the outer and inner supports. In this paper it is assumed that the outer two end support conditions are simply supported and the beam is continuous over the inner supports.

The boundary conditions for this case require that the displacement $\Phi_{nr}(x)$ vanishes at the outer and inner supports as follows:

$$\Phi_{nr}(0) = 0, \quad \Phi_{nr}(l_r) = 0, \quad \Phi_{nr(r+1)}(0) = 0. \tag{10}$$

Eq. (10) gives the boundary conditions of geometric nature and hence represents geometric or essential boundary conditions.

From continuity of the beam over the inner supports, the natural or force boundary condition requires:

$$\begin{aligned} &\frac{\mathrm{d}\Phi_{nr}(x)}{\mathrm{d}x}|_{x=l_r} = \frac{\mathrm{d}\Phi_{n(r+1)}(x)}{\mathrm{d}x}|_{x=0}, \\ &\mathrm{EI}_r \frac{\mathrm{d}^2\Phi_{nr}(x)}{\mathrm{d}^2x}|_{x=l_r} = \mathrm{EI}_{r+1} \frac{\mathrm{d}^2\Phi_{n(r+1)}(x)}{\mathrm{d}^2x}|_{x=0}, \end{aligned} \tag{11}$$

which states that, the slopes and bending moments of two adjacent spans at the common support must be equal.

By substituting the boundary conditions of Eqs. (10) and (11) into (7), the constants A_{nr}, B_{nr}, C_{nr} and D_{nr} can be obtained from the following expressions which are straight forward and easy for computer programming:

For the first span:

$$A_{n,1} = 1, \quad B_{n,1} = 0, \quad C_{n,1} = -\sin \lambda_{n1}L_1 / \sinh \lambda_{n1}L_1, \quad D_{n,1} = 0.$$

For the inner spans:

$$\begin{aligned} B_{n,r+1} &= -\frac{(\lambda_{n,r})^2}{(\lambda_{n,r+1})^2} \times (I_r/I_{r+1}) \\ &\quad \times (-A_{n,r} \sin \lambda_{n,r}L_r - B_{n,r} \cos \lambda_{n,r}L_r + C_{n,r} \sinh \lambda_{n,r}L_r + D_{n,r} \cosh \lambda_{n,r}L_r)/2, \\ D_{n,r+1} &= -B_{n,r+1}, \\ A_{n,r+1} &= -B_{n,r+1}(\cos \lambda_{n,r+1}L_{r+1} - \cosh \lambda_{n,r+1}L_{r+1}) - \frac{\lambda_{n,r}}{\lambda_{n,r+1}} \\ &\quad \times (A_{n,r} \cos \lambda_{n,r}L_r - B_{n,r} \sin \lambda_{n,r}L_r + C_{n,r} \cosh \lambda_{n,r}L_r + D_{n,r} \sinh \lambda_{n,r}L_r) \\ &\quad \times \frac{\sinh \lambda_{n,r+1}L_{r+1}}{\sin \lambda_{n,r+1}L_{r+1} - \sinh \lambda_{n,r+1}L_{r+1}}, \\ C_{n,r+1} &= \frac{\lambda_{n,r}}{\lambda_{n,r+1}} \times (A_{n,r} \cos \lambda_{n,r}L_r - B_{n,r} \sin \lambda_{n,r}L_r \\ &\quad + C_{n,r} \cosh \lambda_{n,r}L_r + D_{n,r} \sinh \lambda_{n,r}L_r) - A_{n,r+1}. \end{aligned}$$

For the last span:

$$
\begin{aligned}
B_{n,r+1} &= -\frac{(\lambda_{n,r})^2}{(\lambda_{n,r+1})^2} \times (I_r/I_{r+1}) \\
&\quad \times (-A_{n,r} \sin \lambda_{n,r}L_r - B_{n,r} \cos \lambda_{n,r}L_r + C_{n,r} \sinh \lambda_{n,r}L_r + D_{n,r} \cosh \lambda_{n,r}L_r)/2, \\
D_{n,r+1} &= -B_{n,r+1}, \\
C_{n,r+1} &= B_{n,r+1}(\cosh \lambda_{n,r+1}L_{r+1}/\sinh \lambda_{n,r+1}L_{r+1}), \\
A_{n,r+1} &= \frac{\lambda_{n,r}}{\lambda_{n,r+1}} \times (A_{n,r} \cos \lambda_{n,r}L_r - B_{n,r} \sin \lambda_{n,r}L_r \\
&\quad + C_{n,r} \cosh \lambda_{n,r}L_r + D_{n,r} \sinh \lambda_{n,r}L_r) - C_{n,r+1},
\end{aligned} \tag{12}
$$

where $n = 1, 2, \ldots$, total number of mode, $r = 1, 2, \ldots$, total number of span, I_r is the second moment of area of the span r, L_r is length of span r.

4. Moving load identification

The response of the system expressed by Eq. (3) can be solved in the time domain by the convolution integral

$$
q_n(t) = \frac{1}{M_n} \int_0^t h_n(t-\tau) p(\tau)\, \mathrm{d}\tau, \tag{13}
$$

where $h_n(t-\tau)$ is the impulse response function and it is given by

$$
h_n(t) = (1/\omega_n') \mathrm{e}^{-\xi_n \omega_n \Delta t(i-j)} \sin(\omega_n' t), \quad t \geqslant 0 \quad \text{and} \quad \omega_n' = \omega_n \sqrt{1-\xi_n^2}. \tag{14}
$$

After substituting Eqs. (13) and (14) into (2) for the generalized coordinate $q_n(t)$, then the dynamic deflection of the beam at point x and time t can be found, as

$$
v(x,t) = \sum_n^{\infty} \frac{\Phi_n(x)}{M_n} \int_0^t (1/\omega_n') \mathrm{e}^{-\xi_i \omega_n (t-\tau)} \sin \omega_n'(t-\tau) \sum_{k=1}^{N_t} p_k(t) \Phi_n(x_k(\tau))\, \mathrm{d}\tau. \tag{15}
$$

4.1. Identification from bending moment

Once if the solution for the deflection is determined using Eq. (15), then the solution for bending moment is simply obtained by applying the relationship of deflection and bending moment from theory of mechanics. Hence, the dynamic bending moment of the beam at point x and time t is given by

$$
m(x,t) = -\mathrm{EI} \frac{\partial^2 v(x,t)}{\partial x^2}. \tag{16}
$$

Substituting Eq. (15) into (16) and assuming that the force $p_k(t)$ is a step function in a small time interval, Eq. (16) can be written in discrete terms as

$$
\begin{aligned}
m(i) &= \mathrm{EI} \sum_n^{\infty} \frac{\Phi_n''(x)}{M_n} \sum_{j=0}^{i} (1/\omega_n') \mathrm{e}^{-\xi_n \omega_n \Delta t(i-j)} \sin \omega_n' \Delta t(i-j) \sum_{k=1}^{N_t} p_k(t) \Phi_n(x_k(\tau)) \\
i &= 0, 1, 2, \ldots, N,
\end{aligned} \tag{17}
$$

where, Δt is the sampling interval and $N+1$ is the number of sample points.

It can be seen that the right-hand side of Eq. (17) consists of two parts, namely, (1) the system associated with the bridge deck and the force, and (2) axle force due to the moving vehicle. Therefore, Eq. (17) can be arranged in matrix form based on the components as follows:

$$
\underset{(N-1)\times 1}{\mathbf{b}} = \underset{(N-1)\times(N_B-1)\,(N_B+1)\times 1}{\mathbf{A}\ \mathbf{x}}, \tag{18}
$$

where, $N_B = l/c\Delta t$ and **b** is the time series vector of the bending moment response, **x** is the time series vector of the time-varying force $\boldsymbol{p}(t)$ to be identified and **A** is the coefficient matrix which is associated with the system of the bridge deck and the force.

4.2. Identification from acceleration

It is shown above that the time-varying force could be identified if the bending moment responses are acquired. Most often the bending moment responses are measured using strain gauges indirectly. The installation of the strain gauges requires substantial work load and time; hence, acceleration measurements are more convenient and easier to conduct than strain gauges. It is, therefore, worthwhile exploring the possibility of force identification from acceleration responses on the continuous bridge.

Again using the same principle as in Section 4.1 the acceleration of the system can be derived from deflection. Hence, the acceleration at point x and time t can be obtained from

$$a(x,t) = \frac{\partial^2 v(x,t)}{\partial t^2} \tag{19}$$

after substituting Eq. (15) into (19). Then we arrive at

$$a(x,t) = \frac{\partial^2 v(x,t)}{\partial t^2} = \sum_n^{\infty} \frac{1}{M_n} \Phi_n(x) \left[p_n(t) + \int_0^t \ddot{h}_n(t-\tau) p_n(\tau)\, \mathrm{d}\tau \right]. \tag{20}$$

Eq. (20) can be written in discrete terms as

$$a(i) = \frac{1}{M_n} \sum_{n=1}^{\infty} \Phi_n(x) \left[\Phi_n(c\Delta t i) p(i) + \sum_{j=0}^{i} \ddot{h}(i-j) \Phi_n(c\Delta t j) p(j) \right]. \tag{21}$$

Eq. (21) can also be expressed in matrix form similar to Eq. (18). In this case **b** stands for the time series vector of the acceleration response, where as the same expressions apply for **x** and **A** as stated in Eq. (18).

Whilst using acceleration responses in the force identification process, the static loads cannot be identified. However, for the comparison of the results with those obtained from bending moment responses the static component of the load is added to the identified dynamic load. It is known that obtaining the acceleration responses could be easier than the bending moment responses as the installation of accelerometers is simpler than that for strain gauges. It is therefore suggested to explore the use of the acceleration responses together with the bending moment responses so that the static component of the load could be determined by the bending moment responses. The number of required strain gauges could then be reduced.

4.3. Identification using responses of the target span

The main purpose of moving force identification is to determine the dynamic axle load history of a moving vehicle so that a better understanding of bridge–vehicle interaction could be obtained. It is not essential to obtain the time history of the axle force for all the spans. Most often, only a typical or a critical span is of interest. For a continuous supported bridge consisting of many spans, is it necessary to instrument all the spans in order to identify the moving forces on a particular span of the bridge? It will be much more efficient and economical if a method is developed to identify the moving forces on a particular span while only this span (the target span) is used.

The bridge response Eqs. (15), (17) and (21) are developed on the basis of considering all the spans of the beam. This means that in order to get the responses due to the external loads, the moving loads should travel from the first entry point of the bridge to the exit point of the bridge. In this approach the efficiency of the method in identifying moving forces becomes worse and more noise sensitive as the number of spans increases. This is because of the fact that the moving force identification is an inverse problem, and the solution of the system mainly depends up on the condition of matrix (in this case matrix A) that to be inverted. And the condition of matrix A mainly depends on the parameters, which generated it. One of these parameters from which matrix A is generated is modal shape functions. No matter how many mode shapes to be considered,

from the boundary conditions given in Eq. (10) it is understood that the value of modal shape functions approaches to zero at the neighbourhood of the supports and turns to be zero at the supports. This will then affect the values of the coefficient matrix A by introducing zero entries periodically in the corresponding elements based on the number of the supports, i.e. as the number of the support increases the number of zero entries will be increased and vice versa is also true. As mentioned earlier, in order to obtain the solution, matrix A should be inverted, and the zero elements in it will bring its ill conditioning which will then become very sensitive for noise. It is a problem that engineers and researchers have to face when carrying out practical measurements in laboratories and in field tests.

In addition, as the number of the span increases, the number of elements in matrix A will also be increased, Therefore, longer computation time is required to obtain the solution because of the longer time needed to invert the big matrix **A** in Eq. (18), which is one of the main drawbacks of the TMD [9,10]. To avoid all the mentioned limitations of moving force identification on continuous bridges, the new approach is developed and introduced using the responses from one span (target span) only to identify the time history of the moving vehicle loads on that span while the vehicle is moving across the whole beam rather than considering all the spans in the analysis of the responses. Since Eq. (7) is derived directly to get the mode shapes of each span, the response Eqs. (15), (17) and (21) can be written as follows to calculate the responses of the specified span,

$$v(x,t)=\sum_{n}^{\infty}\frac{\Phi_{nr}(x_r)}{M_n}\int_0^t(1/\omega_n')\mathrm{e}^{-\xi_i\omega_n(t-\tau)}\sin\,\omega_n'(t-\tau)p(\tau)\Phi_{nr}(x_k(t))\,\mathrm{d}\tau, \tag{22}$$

$$m(i)=\mathrm{EI}\sum_{n}^{\infty}\frac{\Phi_{nr}''(x_r)}{M_n}\sum_{j=0}^{i}(1/\omega_n')\mathrm{e}^{-\xi_n\omega_n\Delta t(i-j)}\sin\,\omega_n'\Delta t(i-j)p(\tau)\Phi_{nr}(x_k(t)), \tag{23}$$

$$a(i)=\frac{1}{M_n}\sum_{n=1}^{\infty}\Phi_{nr}(x)\left[\Phi_{nr}(c\Delta ti)p(i)+\sum_{j=0}^{i}\ddot{h}(i-j)\Phi_{nr}(c\Delta tj)p(j)\right], \tag{24}$$

where Φ_{nr} is the nth modal shape function of the given span r. The responses of the target span under consideration are recorded in a time gap between the first axle of the vehicle load entering the span and the last axle of the vehicle leaving the span. In the moving force identification from the target span only one span is considered so that the number of zero elements in a matrix A is minimized due to reducing zero values of mode shape functions at the support. In addition to increasing the efficiency of the method, this approach also improves the identification accuracy.

The selection of target span for moving force identification from continuous beam is depending up on the user of this method. It means that the method can be applied on any span weather it is the first or last span of the continuous supported bridge of interest. The selection of the target span may be based on the span which is more interesting to study, e.g. showing unusual bridge responses, or it could be based on the installations conditions of sensors, e.g. the under structure condition of one span may be better than others.

4.4. Solution

If $N=N_B$, matrix A becomes a lower triangular matrix and the force vector can be obtained directly by solving Eq. (18). If $N>N_B$, and/or N_1 bending moments or acceleration responses ($N_1>1$) are measured, the least-squares method can be used to find the time history of the moving forces $p(t)$, by directly calculating the pseudo-inverse (PI) of A, $A^+=(A^{\mathrm{T}}A)^{-1}A^{\mathrm{T}}$.

The least-square solution of Eq. (18) is given by Yu and Chan [15] and written as follows:

$$x=A^+b=[(A^{\mathrm{T}}A)^{-1}A^{\mathrm{T}}]b. \tag{25}$$

If A is close to rank deficient then the method of singular value decomposition (SVD) can be applied as successfully used by Yu and Chan [15]. If A is real, the SVD of A is USV^{T}, where, U is an orthogonal $k\times k$ matrix, V is an orthogonal $n\times n$ matrix and S is a real diagonal $k\times n$ matrix in which the elements at the leading diagonal of the matrix are called the singular values of A. The least-squares solution vector x is

then given by

$$x = (VS^{-1}U^{T})b. \tag{26}$$

5. Numerical examples and simulation

5.1. Identification of moving forces from continuous beam

In order to check the correctness of the above-mentioned method, two time-varying moving forces are simulated as follows.

$$\begin{aligned} p_1(t) &= 58.8[1 + 1.0\ \sin(10\pi t) + 0.05(40\pi t)] \quad \text{kN}, \\ p_2(t) &= 137.2[1 - 1.0\ \sin(10\pi t) + 0.05(50\pi t)] \quad \text{kN}, \\ l_s &= 8\,\text{m (axle spacing)}. \end{aligned} \tag{27}$$

The two forces simulate a vehicle with a static gross weight of 200 kN, similar to the one used in Chan et al. [9], with the first and second static forces being 58.8 and 137.2 kN, respectively, and having an 8 m axle spacing. The vehicle is moving with a constant velocity of 30 m/s over the bridge.

The bridge is modelled as a three span continuous beam over two internal supports, and simply supported over the two outer supports. The parameters of the beam are $\text{EI} = 1.279140 \times 10^{11}\,\text{N m}^2$ and $\rho = 1.2 \times 10^4\,\text{kg/m}$. The total length of the beam is 60 m and the length of each of the three spans is 20 m. Damping has been taken to be $\zeta = 0.02$ for all modes. The first five vibration modes are included in the calculation and the corresponding natural frequencies were obtained by the method presented in Ref. [16]. As indicated by Proakis and Manolakis [17] the sampling frequency should be at least two times the highest frequency contained in the signal, which is called Nyquist rate. For this particular case the highest frequency occurred at the fifth natural mode, and from calculation the frequency of the fifth mode was obtained to be 58.45 Hz, and hence the Nyquist rate is two times this value and found to be 116.9 Hz. Any value equal or above this value can be taken as the sampling frequency. In addition the upper limit of the sampling frequency depends upon the computation capacity of the computer used since higher values of sampling frequency need longer computation time. Therefore, the optimum value of 200 Hz is selected as sampling frequency and 512 measuring points are included in the calculation. After obtaining the simulated forces, the simulated bending moment and acceleration responses at different locations of the beam can be calculated using Eqs. (17) and (21), respectively, which are forward problems. White noise is added to the calculated responses to simulate the polluted measurements as follows:

$$\begin{aligned} \mathbf{m} &= \mathbf{m}_{\text{calculated}} + \text{Ep} \times ||\mathbf{m}_{\text{calculated}}|| \times \mathbf{N}_{\text{ois}}, \\ \mathbf{a} &= \mathbf{a}_{\text{calculated}} + \text{Ep} \times ||\mathbf{a}_{\text{calculated}}|| \times \mathbf{N}_{\text{ois}}, \end{aligned} \tag{28}$$

where, Ep is the specified error level, $\mathbf{N}_{\text{ois}}$ is a standard normal distribution vector (with zero mean value and unit standard deviation), **m** and **a** stand for the bending moment and acceleration responses, respectively. For inverse problems during the simulation, the simulated bending moments and accelerations are taken as measured responses of the beam and using these simulated bending moment responses the forces can be identified. To study the inverse problem, the solution method of SVD of the coefficient matrix in the over determined system of equation is used in identifying moving forces. Case studies are carried out on both a continuous beam (considering all spans) and on one selected span of the beam. The middle span is selected as a target span to show the effectiveness of the method in identifying moving forces by considering only one span from the continuous beam model.

To evaluate the method and the identification accuracy, the relative percentage error (RPE) between the true and identified forces are calculated for a different number of sensors with different arrangements as follows:

$$\text{Error} = \frac{\sum |f_{\text{true}} - f_{\text{identified}}|}{\sum |f_{\text{true}}|} \times 100\%. \tag{29}$$

In Eq. (29), the true force is directly obtained from the simulated time-varying moving forces in Eq. (27) and the identified force is obtained from by solving inverse problem as stated in Eq. (26) from the corresponding simulated bending moment or acceleration responses.

Tables 1 and 2 show the RPE results between the true and identified forces under different noise levels from the simulated bending moment and acceleration responses, respectively. Note that for the purpose of comparison of the identified forces obtained from the simulated acceleration responses with that of the bending moment responses the static component of the load is added to the dynamic load obtained from acceleration responses as mentioned in Section 4.2. The comparisons of identified forces for three sensors with 5% noise level in simulated responses are shown in Figs. 3 and 4. From analysis of the above-mentioned tables and figures, the following are noted:

(a) If $Ep = 0$, i.e. no noise is added to the simulated bending moment and acceleration responses, the identified forces are very close to the true forces. This indicates that the identification method and algorithms are correct.
(b) The errors between the identified and true forces increase with the increase of noise level; this shows that the method is noise sensitive. Identified results from acceleration responses are more affected by noise than those obtained from bending moment responses.
(c) As the noise level increases, the RPE values are mostly affected by locations of sensors when bending moment responses are used. For example, as shown in Table 1, when five numbers of sensors are used by locating them at different positions on the beam, different results are obtained. A dramatic increase of RPE is noticed when the five sensors are distributed in all of the three spans. On the other hand, the results from acceleration responses are least affected by location of sensors. From Figs. 3 and 4 for both identified results from bending moment and acceleration responses it is noticed that the big ripples occurred at neighbourhood of the supports indicating the matrix A is very ill conditioned at those regions. This is in good agreement with discussion presented in Section 4.3. It was mentioned in Section 4.3 that the values of

Table 1
RPE values in two forces identification (%) from simulated bending moment responses

No. of sensors	Location of sensors from the left support of the beam in meters	0% Ep		1% Ep		5% Ep	
		Axle 1	Axle 2	Axle 1	Axle 2	Axle 1	Axle 2
3	25 30 35	0.018	0.008	4.869	2.327	24.340	11.630
4	24 28 32 36	0.018	0.007	3.513	1.745	17.564	8.725
5	24 27 30 33 36	0.016	0.006	3.537	1.721	17.689	8.606
5	22.5 25 30 35 37.5	0.016	0.006	3.135	1.538	15.676	7.692
5	10 25 30 35 50	0.014	0.006	18.240	4.910	91.230	24.550
7	10 15 25 30 35 45 50	0.014	0.006	10.107	2.537	50.530	12.680

Table 2
RPE values in two forces identification (%) from simulated acceleration responses

No. of sensors	Location of sensors from the left support of the beam in meters	0% Ep		1% Ep		5% Ep	
		Axle 1	Axle 2	Axle 1	Axle 2	Axle 1	Axle 2
3	25 30 35	0.015	0.006	25.260	9.981	126.312	49.923
4	24 28 32 36	0.015	0.006	23.937	9.516	119.680	47.584
5	24 27 30 33 36	0.013	0.005	24.726	9.791	123.627	48.951
5	22.5 25 30 35 37.5	0.012	0.005	20.990	8.447	104.950	42.231
5	10 25 30 35 50	0.016	0.005	18.848	7.521	94.231	37.612
7	10 15 25 30 35 45 50	0.012	0.005	11.148	4.082	55.735	20.144

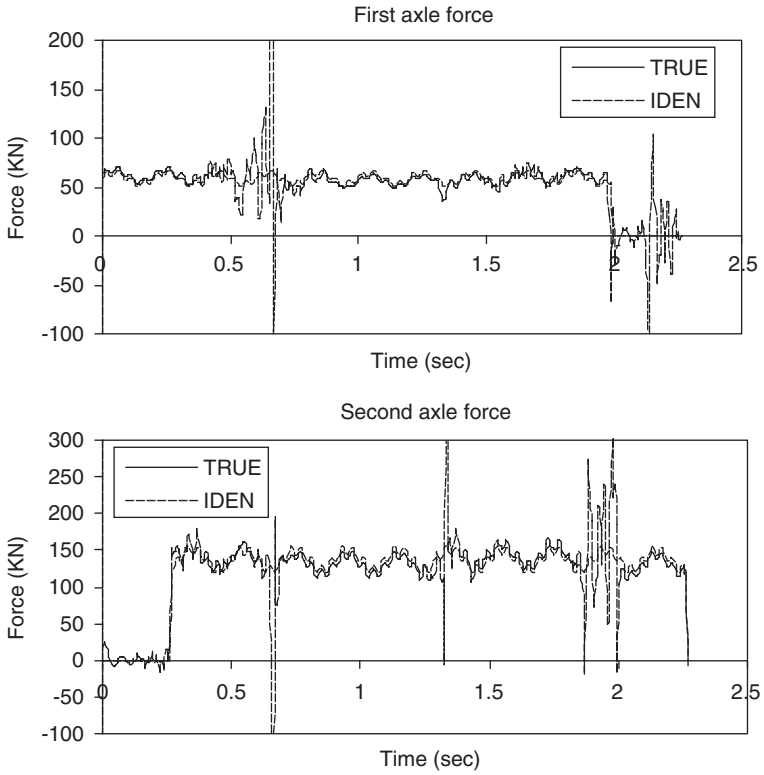

Fig. 3. Identified moving forces with 5% noise in the simulated bending moment responses.

the modal shape functions near the supports are very close to zero, which will then affect the values of the inverse of the of the coefficient matrix **A** in Eq. (18) around the supports. This will bring ill conditioning in the coefficient matrix **A**.

5.2. *Moving force identification using responses from middle span*

The same simulated time-varying two moving forces in Section 5.1 are used. In this case only the response of the middle span of the beam is considered to identify moving time-varying forces in the middle of the span. The time history of the bridge response due to moving forces is obtained from the forward problem starting from the instant at which the simulated first axle force crosses the first support of the span until the instant at which the second axle force leaves the span. The results obtained from error study of force identification for different sensors arrangement are given in Tables 3 and 4.

From the results presented in Tables 3 and 4 and Figs. 5 and 6 the following comments are given on the identification of moving forces from middle span using simulated bending moment and acceleration responses.

(a) If $Ep = 0$, i.e. no noise is added to the simulated bending moment and acceleration responses, the identified forces are very close to true forces. This indicates that the identification method and algorithms are correct.
(b) As the noise level increases, the identified results from acceleration responses are more affected than those results obtained from bending moment responses.
(c) Results obtained from acceleration responses are least affected by different location and arrangement of sensors. However, as seen from Table 3 results from bending moment responses are affected by different locations of sensors for the same number of sensors. Higher RPE values are obtained in the last row of

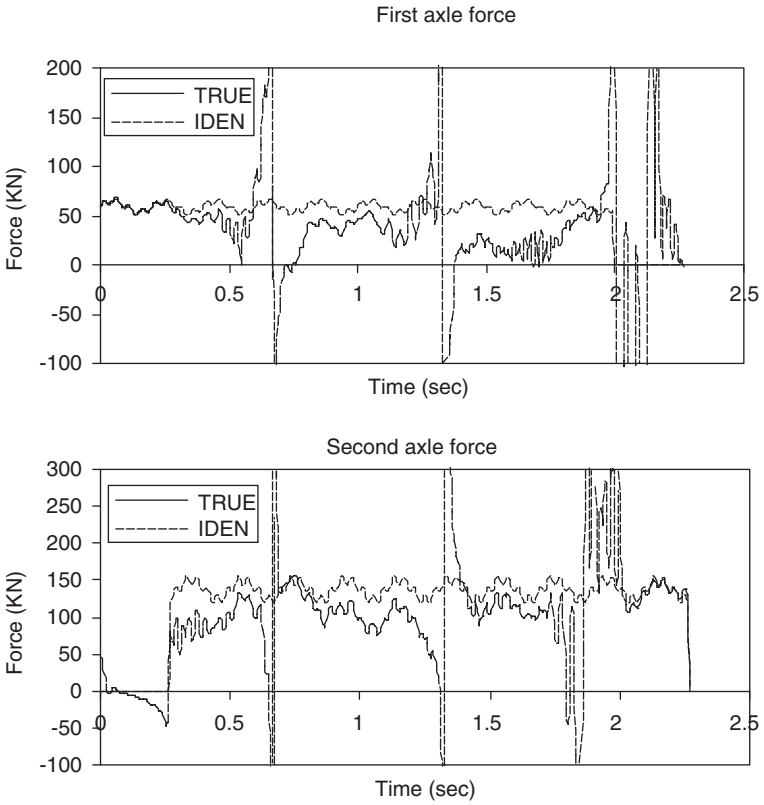

Fig. 4. Identified moving forces with 5% noise in the simulated acceleration responses.

Table 3
RPE values in two forces identification (%) in middle span, from simulated bending moment responses

No. of sensors	Location of sensors from the left support of the beam in meters	0% Ep		1% Ep		5% Ep	
		Axle 1	Axle 2	Axle 1	Axle 2	Axle 1	Axle 2
3	25 30 35	0.017	0.007	1.475	1.160	7.361	5.847
4	24 28 32 36	0.020	0.008	1.382	1.270	6.880	6.322
5	24 27 30 33 36	0.018	0.007	1.261	1.211	6.281	6.064
5	22.5 25 30 35 37.5	0.016	0.006	2.621	1.145	13.121	7.034

Table 4
RPE values in two forces identification (%) in middle span, from simulated acceleration responses

No. of sensors	Location of sensors from the left support of the beam in meters	0% Ep		1% Ep		5% Ep	
		Axle 1	Axle 2	Axle 1	Axle 2	Axle 1	Axle 2
3	25 30 35	0.012	0.005	8.230	3.121	41.151	15.630
4	24 28 32 36	0.011	0.004	8.069	3.012	40.342	15.080
5	24 27 30 33 36	0.015	0.005	8.147	3.095	40.711	15.493
5	22.5 25 30 35 37.5	0.011	0.005	7.781	2.913	39.921	13.572

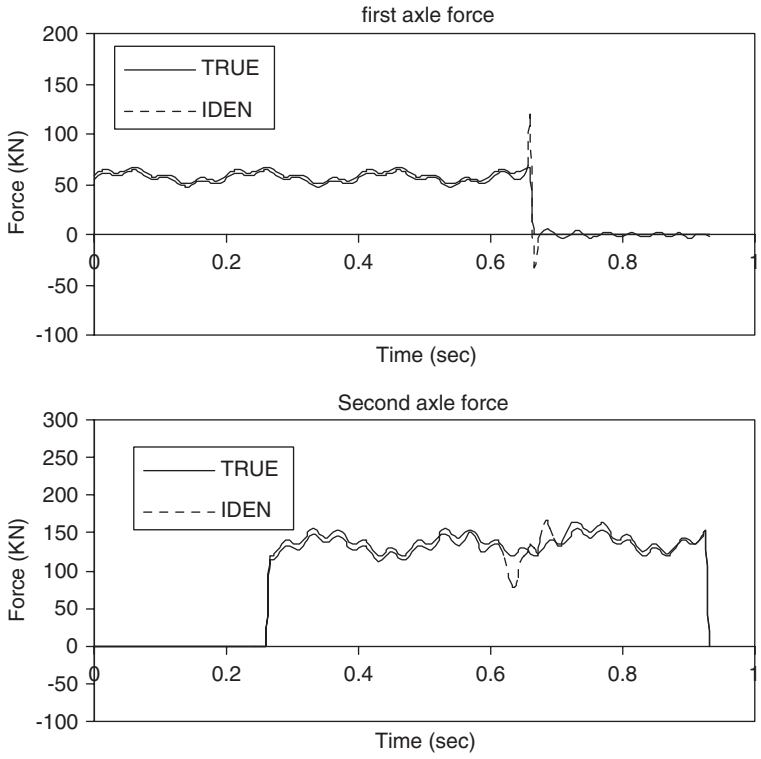

Fig. 5. Identified moving forces from middle span with 5% noise in the simulated bending moment responses.

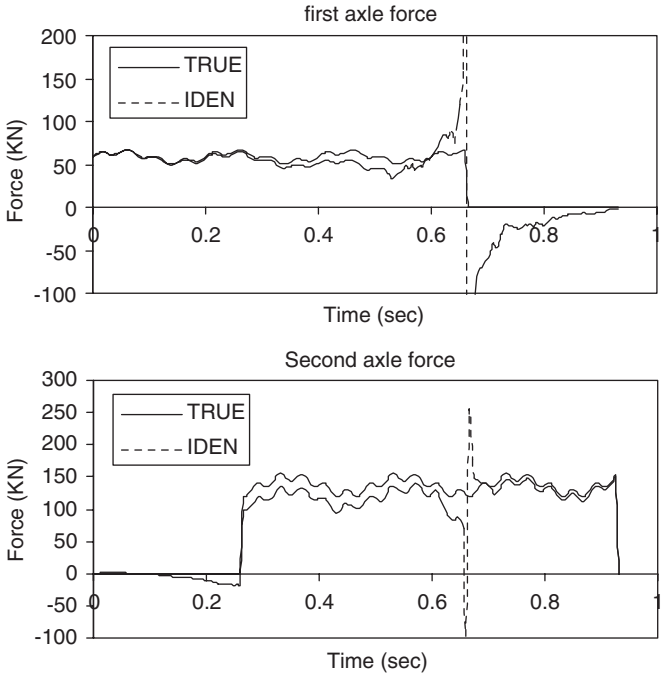

Fig. 6. Identified moving forces from middle span with 5% noise in the simulated acceleration responses.

Table 3 with 5% noise level. This is due the fact that the locations of the two outer sensors are closer to the supports. The moments at which the front axle leaving the target span is the main reason for the big ripples noticed in identified moving force in Figs. 5 and 6. In general, better identification accuracy can be attained when only one span is used in the force identification process.

6. Conclusions

The results presented in this paper indicate that it is possible to identify moving forces from bending moment and acceleration responses on a continuous beam. Good accuracy is attained when the moving force identification is carried out in the absence of noise in simulated responses. The accuracy of identification is lower at the moments when the second axle is entering the beam and the first axle is leaving from the beam. The other locations at which the accuracy of identification is affected the most are locations around the supports. The accuracy of the identified forces becomes lower with the increase of noise level in both the simulated bending moment and acceleration responses, and it has been shown that results from acceleration responses are most affected by noise. A new approach of identifying the interactive forces between the axles and the bridge from the responses of only one span of a continuous bridge is developed while the vehicle is moving across the whole beam, and better identification accuracy is obtained. In addition, when using this method the computation time needed is much lower than considering all spans of the continuous bridge in the force identification process.

Acknowledgement

The work described in this paper was fully supported by a grant from the Research Grants Council of the Hong Kong Special Administrative Region, China (Project No. PolyU 5033/02E).

References

[1] P. Davis, F. Sommerville, Low-Cost Axle Load Determination, *Proceedings of the 13th ARRB & Fifth REAAA Combined Conference*, part 6, 1986, pp. 142–149.
[2] R.J. Peters, AXWAY—a system to obtain vehicle axle weights, *Proceedings of the 12th ARRB Conference*, Vol. 12(2), 1984, pp. 10–18.
[3] R.J. Peters, CULWAY—an unmanned and undetectable highway speed vehicle weighting system, *Proceedings of 13th ARRB & Fifth REAAA Combined Conference*, part 6, 1986, pp. 70–83.
[4] Cebon, D. Assessment of the dynamic wheel forces generated by heavy road vehicles, *Proceedings of the Symposium on Heavy Vehicle Suspension and Characteristics*, Australian Road Research Board, 1987.
[5] T.H.T. Chan, C. O'Connor, Wheel loads from highway bridge strains—field studies, *Structural Engineering ASCE* 116 (1990) 1751–1771.
[6] T.H.T. Chan, S.S. Law, T.H. Yung, X.R. Yuan, An interpretive method for moving force identification, *Journal of Sound and Vibration* 219 (3) (1999) 503–524.
[7] S.S. Law, T.H.T. Chan, Q.H. Zeng, Moving force identification—time domain method, *Journal of Sound and Vibration* 201 (1) (1997) 1–22.
[8] S.S. Law, T.H.T. Chan, Q.H. Zeng, Moving force identification—a frequency–time domains approach, *Journal of Dynamic Systems, Measurement and Control ASME* 121 (3) (1999) 394–401.
[9] T.H.T. Chan, L. Yu, S.S. Law, T.H. Yung, Moving force identification studies I: theory, *Journal of Sound and Vibration* 247 (1) (2001) 59–76.
[10] T.H.T. Chan, L. Yu, S.S. Law, T.H. Yung, Moving force identification studies II: comparative studies, *Journal of Sound and Vibration* 247 (1) (2001) 77–95.
[11] D.Y. Zheng, Y.K. Cheung, F.T.K. Au, Y.S. Cheng, Vibration of multi-span non-uniform beams due to moving loads, *Journal of Sound and Vibration* 212 (3) (1998) 455–467.
[12] K. Henchi, M. Fafard, G. Dhatt, M. Talbot, Dynamic behaviour of multi-span beams under moving loads, *Journal of Sound and Vibration* 199 (1) (1997) 33–50.
[13] Y.A. Dugush, M. Eisenberger, Vibrations of non-uniform continuous beams under moving loads, *Journal of Sound and Vibration* 254 (5) (2002) 911–926.

[14] D. Cebon, *Hand book of Vehicle– Road Interaction*, Sweets & Zeitlinger Publishers, 1999.
[15] L. Yu, T.H.T. Chan, Moving force identification based on the frequency–time domain method, *Journal of Sound and Vibration* 261 (2) (2003) 329–349.
[16] T. Hayashikawa, N. Watanabe, Free vibration analysis of continuous beams with moving loads, *American Society of Civil Engineers, Journal of the Engineering Mechanics* 111 (1985) 639–653.
[17] J.G. Proakis, D.G. Manolakis, *Digital Signal Processing, Principle, Algorithms and Applications*, Prentice-Hall Inc., Englewood Cliffs, NJ, 1996.